Diluted- and Distributed-Absorption Microwave Waveguide Photodiodes for High Efficiency and High Power

Serge Jasmin, Nakita Vodjdani, Jean-Charles Renaud, and Alain Enard

***Abstract*— We propose a new microwave photodetector with high responsivity, which can handle both high optical power and deliver high microwave-output power. The distributed-absorption waveguide photodiode (DWGPD) is specially designed to equally distribute the photocarriers over the maximum surface area available in order to reduce the nonlinearities of electrical response due to electric-field screening effects. The expected calculated performances of this DWGPD is compared to other types of broad-band photodetectors in terms of linear microwave-output power, quantum efficiency, and thermal behavior. The fabricated DWGPD's have a responsivity of 1 A/W, cutoff frequency of 29 GHz, and linear response up to 8 mA limited in this experiment by contacting electrodes.**

***Index Terms*—Microwave photodiodes, nonlinearity, optical RF link, traveling-wavc photodetectors, waveguide photodiodes.**

I. Introduction

HIGH-PERFORMANCE fiber-optics RF links need to meet different specifications together:

1) operate at high frequency;
2) have low input/ouput microwave loss;
3) have large spurious-free dynamic range.

It has been shown that in externally modulated RF fiber-optics links, the link gain and spurious-free dynamic range can be enhanced and the noise figure reduced by increasing the CW laser input power [1]. However, at the receiver side of the link, it is the efficiency and saturation power of the detector which conditions these improvements [2].

The response of conventional surface-illuminated photodiodes is limited by a fixed bandwidth efficiency product due to carrier transit time. This bandwidth efficiency product has been improved by using waveguide detectors [3], and traveling-wave detectors [4]. However, in these structures, the typical absorption length is about 10 μm, leading to very small effective absorbing surfaces with high photogenerated-carrier densities. The photogenerated carriers induce electric-field screening effects, which are the origin of the nonlinear behavior of the microwave photocurrent at high optical-input powers and generation of harmonic distortions. In order to have high bandwidth, high efficiency, and high power capabilities, diluted traveling-wave detectors [5] can be used. Here, we propose and analyze a new waveguide photodiode with distributed absorption which is based on a diluted single-mode waveguide for which the photocarrier's charge density is maintained constant along the whole propagation length of the diode (instead of being exponential as in usual waveguide photodiodes) by controlling and tailoring the modal absorption coefficient $\alpha\Gamma(z)$ along the axis of propagation z. This design applies to lumped waveguide photodiodes as well as traveling-wave photodiodes, and in both cases distributes the photocarriers equally over the maximum-junction surface area available. A drift-diffusion model is used to optimize the electrical behavior of the diluted structures and compare distributed-absorption waveguide photodiode (DWGPD) to different types of other p-i-n photodetectors. It is shown in particular, that for the same active volume it is possible to gain about two orders of magnitude in maximum-output RF power by using a DWGPD structure instead of a conventional large-core absorbing layer WGPD.

Manuscript received December 20, 1996; revised April 23, 1997.

The authors are with Thomson-CSF Research Laboratory (LCR), Domaine de Corbeville 91401, Orsay, France.

Publisher Item Identifier S 0018-9480(97)06004-3.

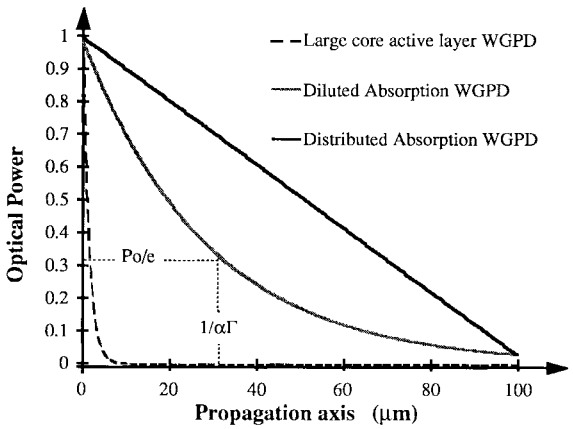

Fig. 1. Optical-power profiles in different p-i-n photodiodes.

II. Principle of Operation—Design Issues

Fig. 1 shows a simple representation of the decrease of the optical power along the waveguide propagation axis for a large-core active-layer WGPD [3], a diluted active-layer WGPD [5], and a distributed-absorption WGPD. The whole intrinsic layer of the large-core active-layer WGPD is an absorbing layer with a thickness limited by transit time. The confinement factor Γ in the active layer is high and, therefore, the absorption length is a few microns leading to very small effective active surfaces and high photogenerated-

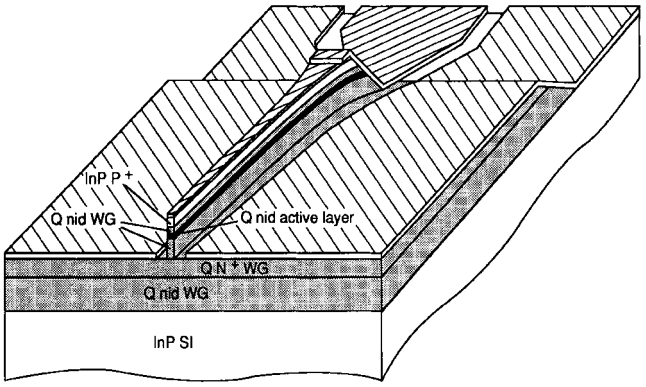

Fig. 2. Perspective view of DWGPD with coplanar electrodes.

carrier density. In diluted WGPD's, the confinement factor of the absorbing layer is reduced by embedding the absorbing layer in a transparent intrinsic layer. The desired effective photodiode (PD) absorption length is obtained by adjusting the thickness of the active layer to obtain the desired confinement-factor Γ. The whole intrinsic layer's thickness is limited by the photocarrier's transit time and is calculated to obtain the wanted cutoff frequency. This permits the reduction of the junction capacitance and device depolarization. The linearity of the PD can be further increased in distributed-absorption WGPD's by *uniformly* distributing photocarriers along the WGPD propagation axis and replacing the exponential optical-absorption decay by a linear decay (Fig. 1). For this, the effective absorption coefficient in the active layer $(\alpha\Gamma(z))$ must progressively increase along the propagation axis. A simple way to do it is represented in Fig. 2 and consists of increasing the width of the WGPD along the propagation axis. When the waveguide width is small compared to its thickness, the mode is pinched. It is weakly confined in the ridge and is mainly located in the slab waveguide. As the ridge gets broader, the lateral confinement increases and the optical mode goes up in the ridge and $\alpha\Gamma(z)$ increases. The optical mode is calculated by using the Galerkin two-dimensional (2-D) spectral-index method [6]. The calculated mode distribution in the beginning and end of the DWGPD are shown in Fig. 3. The structure is monomode and the modal absorption coefficient $\alpha\Gamma(z)$ can vary by a factor of 10 by changing the ridge width from 2 to 4 μm. The calculated coupling efficiency with a lensed fiber for this structure is 80% for the DWGPD structure and 90% for the same 4-μm-wide untapered structure. The depleted region is constituted of a thin active layer sandwiched between two transparent $Ga_xIn_{1-x}As_yP_{1-y}$ undoped layers lattice matched to InP. This intrinsic zone is located in a waveguiding p-i-n structure, itself embedded in a thicker undoped asymmetric waveguide. Fig. 2 represents the coplanar electrodes configuration adopted for both lumped and traveling-wave structures.

III. Optimization of Maximum-Output Power of Diluted and Distributed Waveguide Detectors

The behavior of the different PD's under illumination is calculated by using a static drift-diffusion model which takes into account the space-charge effects, the heterointerface discontinuities, the device depolarization due to current flow in the load circuit, and the doping level of the intrinsic layer [7]. In order to evaluate the maximum undistorted output power delivered by the PD in the dynamic regime, the calculation was restricted to the linear regime, which here is the optical-power range for which the internal electric field is always below 250 kV/cm (limit of breakdown voltage) and above 50 kV/cm. For this electric-field domain, provided that the depleted region thickness is smaller than $L/2V_{\rm sat}$ and for device dimensions with no *R–C* limitations, the dynamic and static responsivity of the PD are the same. In this regime, electrons and holes reach their saturation velocity in $Ga_xIn_{1-x}As$: $V_n = V_p = V_{\rm sat} = 6.10^6$ cm $\cdot$ s^{-1}. For electric fields under 50 kV/cm, the carriers velocity is not constant anymore, therefore, dynamic nonlinearities occur. The reverse bias and input optical power are varied in order to calculate the maximum linear-RF output power. The maximum linear-RF output power obtained for the same diodes by this model was compared to the one obtained using dynamic-simulation approaches [8] and to experimental data on surface-illuminated PD's, and were found to be in reasonable agreement. Table I is a comparison of the maximum average photocurrent delivered by five different types of structures having all the same active volume, inserted in a different type of intrinsic layers. Structures a and e have an intrinsic layer which is totally absorbing. Their maximum deliverable linear current is 11 mA and is limited by space-charge effects. As shown in Table I, diluted waveguides allow for an increase of the maximum current to 36 mA, while the dilution and equal distribution of carriers along the propagation length allows for a maximum current of 90 mA. The influence of bandgap discontinuities (between the absorbing and transparent layers of the intrinsic zone) on space-charge buildup can be evaluated by comparing the results for structures c and d. From Table I, it can be concluded that while using the same active volume, it is possible to change the maximum-output power by more than two orders of magnitude by using the maximum absorbing surface and depleted thickness. The position of the absorbing layer in the depleted is also optimized. The maximum average photocurrent of a diluted structure of 1.5-μm intrinsic zone and a 0.06-μm active layer decreases from 88 mA for the absorbing layer placed at the P^+ interface to 29 mA in the case of the active layer placed close to the N^+ interface.

The proposed lumped DWGPD and traveling-wave DWPD's structures are compared with conventional surface-illuminated PD's and large-core active-layer WGPD's. The ratio of the maximum microwave power to the required incident optical power $F\,(F = P_{\rm rf\,out}/P_{\rm opt\,in})$ is considered as the figure-of-merit of the performances of the photodiodes, and is reported in Fig. 4 versus cutoff frequency. For each cutoff frequency, the depleted-region thickness is set at its maximum, which is limited by transit time, and then the largest surface junction defined by *R–C* time limitation is used. The best figure-of-merit for each cutoff frequency is obtained by calculating the minimum and maximum of the total electric field in the depleted region for each optical power P_o. The maximum optical power for which 50 kV/cm $< E_{\rm tot\,min}$ and $E_{\rm tot\,max} < 250$ kV/cm is used to calculate the factor-of-merit

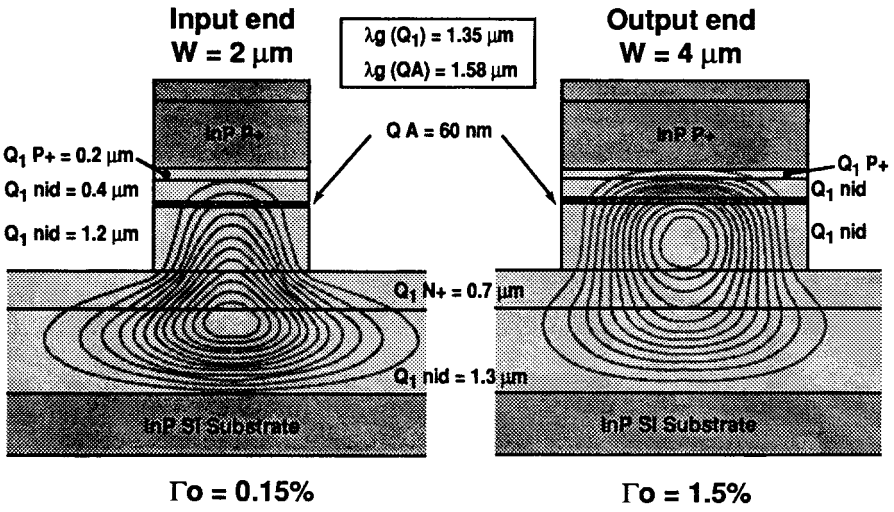

Fig. 3. Cross sections of the input and output ends of the DWGPD, together with the field profiles of the fundamental TE mode calculated using a Galerkin 2-D spectral method.

TABLE I
COMPARISON OF THE MAXIMUM CURRENT DELIVERED BY FIVE DIFFERENT TYPES OF WGPD's HAVING ALL THE SAME ACTIVE VOLUME (120 μm^3), INSERTED IN DIFFERENT TYPES OF INTRINSIC LAYERS

Structure	e_{ZI} (μm)	e_{Active} (μm)	S_{Active} (μm^2)	Imax (mA)	Vmax (V)
(a) Large core	1,5	1,5	80	11	-15,5
(b) Diluted ΔEv = 81 ΔEc = 54 mev	1,5	0,06	2000	36	-16,5
(c) Diluted+ Distributed ΔEv = 81 ΔEc = 54 mev	1,5	0,06	2000	90	-16,5
(d) Diluted+ Distributed ΔEv = ΔEc = 0 mev	1,5	0,06	2000	144	-20
(e) Thin core	0,06	0,06	2000	11	-0,2

F. For traveling-wave DWGPD's, we have taken a junction surface five times larger that the corresponding *R–C* limited maximum surface (to avoid space-charge effects). The aim of this comparison is not to accurately calculate the maximum linear-output power as a function of cutoff frequency, but to analyze the electrical behavior of each type of PD as a function of cutoff frequency. For all structures, we have assumed 100% coupling efficiency and $\alpha = 0,7\ \mu m^{-1}$. As a general trend, for all types of p-i-n photodiodes, there is an asymptotic limitation of the output electrical power at high frequencies due to external depolarization. When the frequency rises, the active layer gets thinner (limited by time transit) and as a consequence, the maximum-allowed bias voltage limited by avalanche breakdown conditions decreases. The effect of device depolarization due to current flow in the load circuit is then increased. This is a material intrinsic limitation—the use of a higher energy gap material would allow for higher electric-field breakdown values and higher maximum-output powers. The difference between the maximum-output power for traveling-wave and lumped DWGPD is due to space-charge effects. The surface-illuminated PD's and lumped DWGPD have the same maximum-output power, since they have the same absorbing surface (*R–C* limited) and same depleted-region thickness. However, the difference between these two structures is significant when considering, internal quantum efficiency, and is well illustrated by the difference in factor-of-merit values. In surface-illuminated PD's the internal quantum efficiency drops when frequency increases, and it is then necessary to inject higher optical power to obtain the same output electrical power. At very high frequencies, large-core active-layer WGPD's tend to the same limit maximum-output electrical power than lumped DWGPD because the thinner active layer dilutes photocarriers over a larger absorption surface which reduces space-charge effects. Finally, it can be noticed that by using DWGPD's for frequencies between 10 and 40 GHz, one can gain two orders of magnitude on maximum-output power and factor-of-merit compared to large core WGPD's. In all cases, the traveling-wave DWGPD has, by far, the best figure-of-merit. Typical calculated maximum-output currents are of the order of 150 mA for −15-V bias voltages. With such high bias voltages and currents, the electrical power dissipated in the device is a few watts. It will, therefore, be the thermal behavior of the device that will limit the high-power performances [9]. The thermal impedance of the different structures is calculated and compared in [7].

IV. FABRICATION AND FIRST EXPERIMENTAL RESULTS

The epitaxial layers of the structure are designed to realize in the same run lumped diluted WGPD's and lumped distributed-absorption DWGPD's. The structure as represented in Fig. 3 is grown on a semi-insulating InP substrate by low-pressure

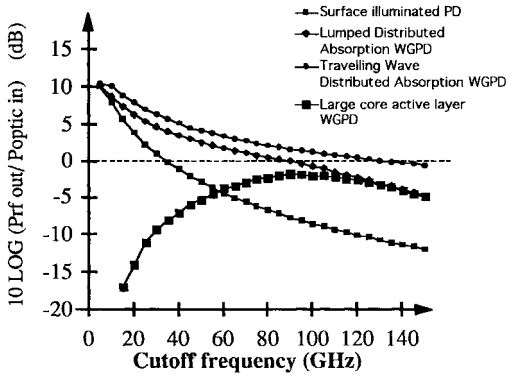

Fig. 4. Ratio of maximum RF output power on optical-input power as a function of cutoff frequency for different types of photodiodes.

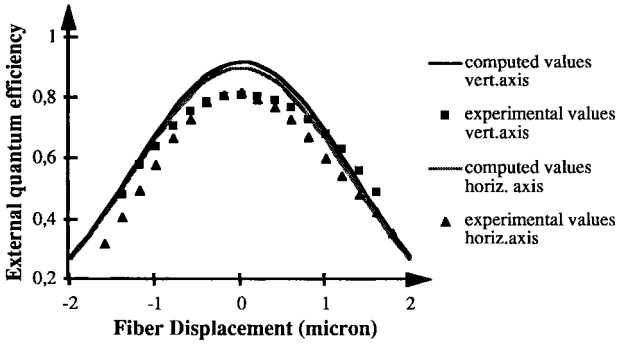

Fig. 5. Experimental and calculated external quantum efficiency and tolerances toward lensed fiber ($w(1/e^2) = 2$ μm) misalignment. Ridge width of 4 μm.

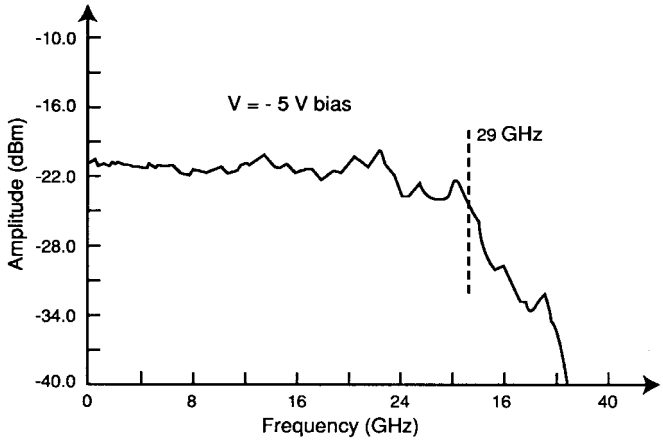

Fig. 6. Measured frequency response of a diluted WGPD corresponding to structure of Fig. 3. Ridge width = 4 μm, length = 120 μm.

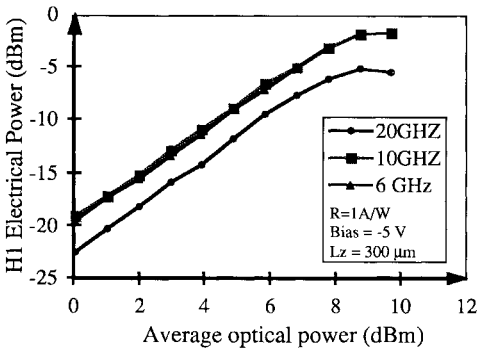

Fig. 7. Measured fundamental harmonic H1 of a 300-μm-long DWGPD as a function of the average optical-input power, at 6, 10, and 20 GHz.

metal organic vapor deposition (LP-MOCVD). The ridge is defined using reactive ion etching (RIE) and a chemical etching process using the Pt/Cr/Au/Cr metallization for p^+ contact and a self-aligned technology. The coplanar n^+ contacts are realized with Au metallization. The electrode geometry adopted for both lumped and traveling-wave structures is designed to have a 50-Ω characteristic impedance and to be compatible with millimeter-wave monolithic microwave integrated circuits (MMIC's) and on chip microwave measurements (Fig. 2). Finally arrays of DWGPD's are cleaved and AR coated. The devices exhibit a dark current of approximately 1 μA and a breakdown voltage of -25 V. For this technological run the devices have a high anomalous serial resistance, which is attributed to the contacting of the top electrode to the coplanar lines. The devices exhibit a responsivity of 1 A/W at a wavelength of 1.532 μm, which corresponds to a coupling efficiency of 81%. Fig. 5 is the external quantum efficiency as a function of fiber displacement. The tolerance is due to the roughly circular large mode of this single-mode photodiode. These experimental values agree well with those predicted by the Galerkin 2-D spectral-index method (Fig. 3). DWGPD's of lengths above 200 μm have a flat optical responsivity as a function of input wavelength in the 1480–1560-nm explored range. The frequency response of a 120-μm-long diluted photodiode have been measured by using an optical heterodyning experiment at 1.55 μm and is represented in Fig. 6. The measured electrical bandwidth for this device is 29 GHz. Fig. 7 is the measured fundamental harmonic H1 of a 300-μm-long DWGPD as a function of the average optical-input power, at 6, 10, and 20 GHz for a -5-V applied bias. This device has a *R–C* limited cutoff frequency of about 20 GHz. It can be seen that it delivers linear microwave photocurrent up to 8 mA at 20 GHz. The devices were damaged for average dissipated powers between 50 and 70 mW. This is the reason why despite the -25-V breakdown voltage, the linearity measurements at high currents could not have been performed at higher voltages. It should be noticed that for our intrinsic layer thickness of 1.66 μm, at -5 V even the dark electric field is much lower than 50 KV/cm, therefore, the roll-off at 8 mA is normal. We observe that when the photodiodes are damaged under high current, it is the contacting zone from top electrodes to coplanar lines which is broken and this creates an *open* circuit unlike large-core WGPD's where a short circuit is observed when damaged. Therefore, the DWGPD's are not destroyed and experimental power limitation is not due to an avalanche breakdown. When the contacting problem will be solved, the expected maximum linear current from calculation for this structure should be around 90 mA (for a bias of -16 V).

V. Conclusion

A new broad-band microwave waveguide photodiode with distributed absorption is proposed. It has high coupling and

quantum efficiencies and can handle both high optical and electrical power. The calculated performances of this lumped and traveling-wave DWGPD's are compared to other types of PD's by using a steady-state drift-diffusion model restricted to the linear regime. From this comparison it can be concluded that by using lumped DWGPD's for frequencies between 10 and 40 GHz, one can gain on maximum-output power compared to large-core WGPD's, and on the responsivity compared to surface-illuminated PD's. In all cases, the traveling-wave DWGPD has, by far, the best figure-of-merit and its power limitation at high frequency depends only on the avalanche breakdown voltage of the material used in the PD intrinsic layer. Experimental results show a high external quantum efficiency of 1 A/W, flat responsivity as a function on wavelength in the 80-nm range explored, cutoff frequency of 29 GHz, and linear response up to 8 mA (-5 V) at 20 GHz. The power limitation is due to technological problems in the contacting electrodes and should be overcome.

ACKNOWLEDGMENT

The authors would like to acknowledge Dr. B. Vinter and Dr. E. Ducloux for fruitful discussions and advice.

REFERENCES

[1] M. L. Farwell, W. S. C. Chang, and D. R. Huber, "Increased linear dynamic range by low biasing the Mach Zehnder modulator," *IEEE Photon. Technol. Lett.*, vol. 5, pp. 779–782, July 1993.

[2] K. J. Williams, R. D. Esman, and M. Dagenais, "Effects of high space charge fields on the response of microwave photodetectors," *IEEE Photon. Technol. Lett.*, vol. 6, pp. 639–641, May 1994.

[3] K. Kato *et al.*, "110 GHz, 50% efficiency mushroom mesa waveguide p-i-n photodiode for a 1.55-μm wavelength," *IEEE Photon. Technol. Lett.*, vol. 6, pp. 719–721, June 1994.

[4] K. S. Giboney *et al.*, "Travelling wave photodetectors with 172-GHz bandwidth and 76-GHz bandwidth-efficiency product," *IEEE Photon. Technol. Lett.*, vol. 7, pp. 412–414, Apr. 1995.

[5] V. M. Hietala, G. A. Vawter, T. M. Brennanand, and B. E. Hammons, "Traveling-wave photodetectors for high-power, large-bandwidth applications," *IEEE Trans. Microwave Theory Tech.*, vol. 43, pp. 2291–2298, Sept. 1995.

[6] D. Marcuse, "Solution of the vector wave equation for general dielectric waveguides by the Galerkin Method," *IEEE J. Quantum Electron.*, vol. 28, pp. 459–465, Feb. 1992.

[7] S. Jasmin, A. Enard, J. Renaud, and N. Vodjdani, "High speed, high power waveguide photodiode with distributed absorption," in *Photonics and Radiofrequencies*. Denver, CO: Spie, 1996.

[8] M. Dentan and B. D. Cremoux, "Numerical simulation of the nonlinear response of a p-i-n photodiode under high illumination," *J. Lightwave Technol.*, vol. 8, pp. 1137–1144, Aug. 1990.

[9] J. Paslaski, P. C. Chen, J. S. Chen, and N. Bar-Chaim, *High Power Microwave Photodiode for Improving Performance of RF Fiber Optic Links in Photonics and Radio Frequencies*. Denver, CO: SPIE, 1996.

Serge Jasmin, photograph and biography not available at the time of publication.

Nakita Vodjdani, photograph and biography not available at the time of publication.

Jean-Charles Renaud, photograph and biography not available at the time of publication.

Alain Enard, photograph and biography not available at the time of publication.